JOURNAL OF SPACECRAFT AND ROCKETS
Vol. 39, No. 1, January–February 2002

Design Considerations When Using Edge-Mounted Heat Pipes in Space Radiators

Todd William Moss* and W. Jerry Bowman†
Brigham Young University, Provo, Utah 84602-4201

An effort to create a design tool for the evaluation of potential heat-pipe fin designs, specifically for flat-plate heat-pipe fins used as space radiators, has been carried out. The axial temperature distribution along the fin was derived using an energy balance. The solution to the differential equation for the temperature distribution was found using the finite difference method. From this solution, the heat transfer from the fin was found, and the efficiency of the fin was calculated. The resulting efficiencies were then plotted as design charts based on the critical parameters. When compared to experimental results of four different tests from the literature, the model yielded good results. The fin model was also used to consider improvements to existing satellites. The Viking 1 and 2 orbiters, each with a SNAP-19 radioisotope thermal generator, were studied.

Nomenclature

A = conduction area
C_α = heat absorbed by fin surface, W/m^2
C_ε = radiation constant of fin, W/(m$^2 \cdot$ K^4)
h_i = convection coefficient, inside of fin, W/(m$^2 \cdot$ K)
k = thermal conductivity, W/(m $\cdot$ K)
k_{eff} = effective thermal conductivity of wick, W/(m $\cdot$ K)
L = position along axial length of fin, m
L_h = length of fin, m
L_w = fin width, m
n = numerical special index
q = fin heat transfer, W
T = fin temperature, K
T_h = fin base temperature, K
T_v = vapor temperature within heat pipe, K
t_w = wick thickness, m
Z = nondimensional temperature
Z_v = nondimensional vapor temperature
δ_h = thickness of fin, m
δ_v = thickness of vapor space, m
$\varepsilon_{a,b}$ = emissivity of fin, sides a and b
ζ_{HP} = profile number of fin
η = fin efficiency
σ = Stefan–Boltzmann constant, 5.87×10^{-8} W/(m$^2 \cdot$ K^4)
ω = nondimensional position

Introduction

WITH the increase in electronic capabilities has come an increase in thermal management requirements for electronic components. Rapid heat dissipation prevents overheating in the components, ensuring that the electronics function according to specifications in the design. Because of their high technology status and inaccessibility on operation, satellites have been prime candidates in the past for innovations in reliable thermal management techniques. Heat pipes have been used as cooling devices in satellites for decades; since their development in 1964 (Ref. 1), heat pipes have found numerous applications in space systems.[2–7] Terrestrial applications have also been developed, with heat pipes being used as heat sinks in notebook computers, preheat heat exchangers in combustion processes, temperature and humidity regulators in heating, ventilation, and air conditioning systems, and permafrost temperature regulators in pipelines.[1,8–10] Recent research has focused on heat-pipe penetration into areas previously dominated by solid conduction thermal management devices.[11,12]

Currently, design methods exist that allow the thermal designer to predict accurately the performance of heat pipes based on criteria such as boiling limitations, sonic limitations, etc.[1,8–10] It has been shown that, in many situations, heat-pipe fins outperform standard cooling fins in convective terrestrial environments.[8,11–13] Additionally, other design methods have been developed that model the performance of solid standard fins as radiators in an outer-space environment.[14] However, little empirical work has been reported comparing heat pipe fins and standard fins in purely radiative environments. A design tool that could predict heat-pipe fin performance in outer space would be a time- and money-saving asset to the designer.

Mackay[14] has written extensively on standard fin radiators in outer space. A solid, rectangular profile radiator was modeled, and the following assumptions were made in the analysis: first, the temperature along the hot edge of the extended surface is uniform and constant; second, the flow of heat is in straight lines from the hot to the cold edge of the surface (these lines are normal to the hot edge); third, heat leaves the surface by radiation from the two large surfaces only (no heat is radiated from the edges); fourth, the emissivity ε of the surfaces and the conductivity k of the fin material are independent of variations in temperature; fifth, heat radiates from the surfaces in accordance with the Stefan–Boltzmann law; and sixth, steady-state operation is assumed.

Mackay's[14] results yield heat transfer, fin effectiveness, optimum weight configurations, and design curves. Finally, a step-by-step design procedure is given for rapid evaluation of design options. This comprehensive method will be expanded for the proposed flat-plate heat-pipe fin model and will provide a basis for comparison of a standard fin with results from the new model.

Thus, a flat-plate heat-pipe fin (FPHPF) as a radiator in an outer-space environment will be studied, culminating in the creation of a design tool to aid in conceptual heat-pipe fin development and analysis. Results will yield the following information: temperature distribution, fin efficiency, and results from case studies. The final thrust of the project involves experimental validation of the design tool, comparing experimental data from the literature with theoretical performance.

Governing Equations

Models have been developed that characterize the behavior of heat-pipe fins based on fin geometry and material properties in a convection environment.[15] That analysis was based on assumptions of 1) a straight fin with uniform cross section along the axial

Received 2 January 2001; revision received 27 June 2001; accepted for publication 8 July 2001. Copyright © 2001 by the American Institute of Aeronautics and Astronautics, Inc. All rights reserved. Copies of this paper may be made for personal or internal use, on condition that the copier pay the $10.00 per-copy fee to the Copyright Clearance Center, Inc., 222 Rosewood Drive, Danvers, MA 01923; include the code 0022-4650/02 $10.00 in correspondence with the CCC.

*Research Assistant, Department of Mechanical Engineering.
†Associate Professor, Department of Mechanical Engineering. Senior Member AIAA.

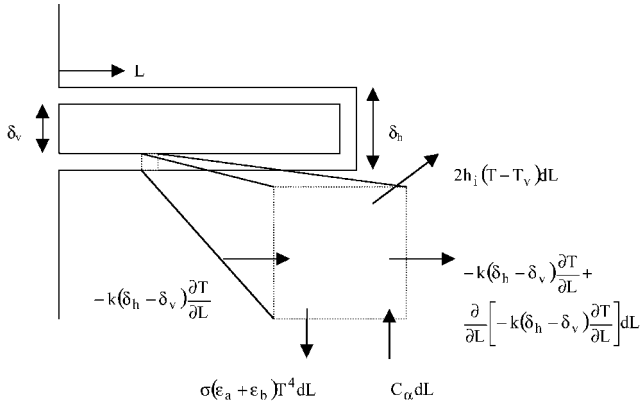

Fig. 1 Schematic of energy equation for FPHPF.

length of the fin, 2) an adiabatic tip condition, 3) an interior convection coefficient h_i being constant, 4) a constant vapor temperature, 5) constant material properties, 6) evaporation from the base area of the heat pipe neglected, and 7) steady-state conditions.

The present analysis is also based on the additional assumptions of 1) an outer-space irradiation environment and 2) a known solar flux (radiant solar energy incident on the FPHPF).

Notation throughout this work reflects the same terminology used in Mackay's work.[14] This convention was chosen to allow ease of comparison between established work in the field and the present research.

Figure 1 gives a schematic of the control volume and energy terms crossing the control surface applied to the FPHPF. The term on the left of Fig. 1 is energy entering the control surface via conduction. On the far right of Fig. 1 is the term representing energy leaving the control surface by conduction. The topmost term is the energy convected to the vapor space. This term is positive where vapor evaporates due to axial conduction of heat from the heat source from the base of the fin. It changes to negative farther along the fin, where the wall temperature is lower than the vapor temperature. After the vapor condenses, it is assumed to return to the evaporator by capillary action to complete the cycle. A model of the liquid return process is not included. The two terms on the bottom of Fig. 1 represent energy leaving the control surface as emitted radiation and energy entering the control surface as environmental radiation.

When combining the Fig. 1 equations on a differential length basis, it can be shown that

$$\left[\sigma(\varepsilon_a+\varepsilon_b)T^4+2h_i(T-T_v)-C_\alpha\right]\mathrm{d}L=k\frac{\mathrm{d}}{\mathrm{d}L}\left[(\delta_h-\delta_v)\frac{\mathrm{d}T}{\mathrm{d}L}\right]\mathrm{d}L \tag{1}$$

where δ_v is the thickness of vapor space of the FPHPF; k is the thermal conductivity of fin material; and T_v is the vapor temperature within heat pipe, $h_i=k_{\mathrm{eff}}/t_w$. C_α is the environmental radiation incident on the fin from the sun and reflected planetary radiation.[14] The internal convection coefficient h_i was assumed to be constant along the fin, both in the evaporator and in the condenser. It is felt that this is a valid assumption because the coefficient is dominated by the thermal resistance through the heat-pipe wick. For a heat pipe with a uniform wick thickness, this thermal resistance will also be uniform.

With Mackay's terminology,

$$C_\varepsilon=\sigma(\varepsilon_a+\varepsilon_b),\qquad Z=T/T_h,\qquad \omega=L/L_h \tag{2}$$

Equation (1) can be simplified to

$$\frac{\mathrm{d}^2Z}{\mathrm{d}\omega^2}-\zeta_{\mathrm{HP}}[Z^4+\mathrm{HPP}(Z)]=-\zeta_{\mathrm{HP}}[\mathrm{HPP}(Z_v)+\mathrm{EP}] \tag{3}$$

where the heat pipe parameter (HPP) is

$$\mathrm{HPP}=2h_i\big/C_\varepsilon T_h^3 \tag{4}$$

the profile number is

$$\zeta_{\mathrm{HP}}=\frac{C_\varepsilon T_h^3L_h^2}{k(\delta_h-\delta_v)} \tag{5}$$

and the environmental parameter (EP) is

$$\mathrm{EP}=C_\alpha\big/C_\varepsilon T_h^3 \tag{6}$$

Equation (3) can be solved to obtain the axial temperature distribution along the heat pipe. HPP includes convection within the vapor space (due to evaporation) and heat radiated away as waste heat from the surface of the fin and ζ_{HP} is the ratio of emitted radiation to axial conduction along the fin. EP represents the ratio of environmental irradiation into the fin to the heat radiated away from the surface of the fin.[14]

The equation was solved using finite difference methods. The finite difference form of the Eq. (3) is

$$(Z_{n+1}-2Z_n+Z_{n-1})\big/\Delta\omega^2-\zeta_{\mathrm{HP}}Z_n^4-\zeta_{\mathrm{HP}}\mathrm{HPP}Z_n$$
$$=-\zeta_{\mathrm{HP}}[\mathrm{HPP}(Z_v)+\mathrm{EP}] \tag{7}$$

When Eq. (7) is solved for Z_n, it yields the nondimensional fin temperature at the nth node in the network. The boundary conditions used were $T(0)=T_h$ and $\mathrm{d}Z/\mathrm{d}\omega(1)=0$.

The dimensionless vapor temperature Z_v is assumed to be constant for any specific heat pipe. It is, however, a function of the dimensionless fin temperature Z for the specific heat pipe. Bowman et al.[15] have shown that, for a constant convection coefficient inside the heat pipe, the average temperature difference between the vapor and the wall must be equal zero. This satisfies the conservation of energy applied to the vapor space. The energy added to the vapor space in the evaporator where the wall is hotter than the vapor must equal the energy removed in the condenser where the wall is cooler than the vapor. Expressed in terms of the dimensionless variables, the dimensionless vapor temperature is the average of the dimensionless fin wall temperature over the length of the fin:

$$Z_v=\int_0^1 Z\,\mathrm{d}\omega \tag{8}$$

Written in finite difference form using the trapezoidal method of integration, Eq. (8) becomes

$$Z_v=\Delta\omega\left(\frac{Z_1}{2}+\sum_{n=2}^{n\max-1}Z_n+\frac{Z_{n\max}}{2}\right) \tag{9}$$

Equations (7) and (9) were solved for $Z_n(\omega)$.

Once the axial temperature distribution is known, the heat transfer from the fin can be determined. Two methods will be discussed. The first method involves taking the base of the FPHPF as a control surface and examining the energy conducted across the surface. The second method consists of determining the net energy leaving the entire fin surface due to radiation.

The first method is simply Fourier's law of conduction at the control surface, as follows:

$$q=-kA\frac{\mathrm{d}T}{\mathrm{d}L}\bigg|_{L=0}=\frac{-kL_w(\delta_h-\delta_v)T_h}{L_h}\frac{\mathrm{d}Z}{\mathrm{d}\omega}\bigg|_{\omega=0} \tag{10}$$

or, in finite difference form,

$$q=\frac{-kL_w(\delta_h-\delta_v)T_h}{L_h}\frac{Z_2-Z_1}{\Delta\omega} \tag{11}$$

where Z_1 and Z_2 are nondimensional temperatures of the first and second nodes in the network, from the base.

The second method involves integrating the radiation loss over the surface of the fin, thus giving heat rejected by the fin. However, the environmental solar flux is a heat in term (from the sun, for example) and must be accounted for in the net heat transfer:

$$q = C_\varepsilon L_w \int_0^L T^4 \, dL - C_\alpha L_w L_h$$

$$= C_\varepsilon L_w L_h T_h^4 \int_0^1 Z^4 \, d\omega - C_\alpha L_w L_h \quad (12)$$

In finite difference form, again using the trapezoidal integration method, the yield is

$$q = C_\varepsilon L_w L_h T_h^4 \Delta\omega \left(\frac{Z_1^4}{2} + \sum_{n=2}^{n\max - 1} Z_n^4 + \frac{Z_{n\max}^4}{2} \right) - C_\alpha L_w L_h \quad (13)$$

Regardless of the method used to determine heat transfer, the efficiency of any fin is the actual heat transfer from the fin divided by the maximum heat transfer if the entire fin were at the fin's base temperature, or

$$\eta = q/q_{\max} \quad (14)$$

The maximum heat transfer is

$$q_{\max} = C_\varepsilon L_w L_h T_h^4 \quad (15)$$

For the conduction through the base method [Eq. (11)], the efficiency may be simplified to

$$\eta = -(1/\zeta_{HP})[(Z_2 - Z_1)/\Delta\omega] \quad (16)$$

For the efficiency of the fin by the integration of the radiation loss [Eq. (13)],

$$\eta = \Delta\omega \left(\frac{Z_1^4}{2} + \sum_{n=2}^{n\max - 1} Z_n^4 + \frac{Z_{n\max}^4}{2} \right) - \mathrm{EP} \quad (17)$$

With the efficiencies from both methods known, it becomes necessary to determine the size of the nodal network to be used and the degree of error to which the numerical solution deviates from the exact solution. One method of quantifying the error is comparing efficiency for various nodal network sizes. For this study, cases at profile number $\zeta_{HP} = 0.5$ and 3 were examined at EP of 0–0.9.

Dozens of studies were conducted to determine convergence of the two efficiency methods. Because all of the results led to the same conclusion, only a small sampling of the results is given. The following descriptions summarize the error analysis.

Figure 2 simulates a condition similar to a satellite's FPHPF, where environmental radiation incident on the fin may be neglected. When the integration method was used (finding the radiation leaving the fin surface), the difference between the efficiency using 40 and 480 nodes was 0.29%. The conduction energy transfer through the base of the fin was more dependent on the numerical grid, as can be seen from Fig. 2.

Figure 3 includes additional effects of environmental radiation incident on the fin, reflected in an environmental parameter of 0.9 (or the incident environmental radiation equal to 90% of the radiation rejected by the fin). At this low efficiency, the difference between 40 and 320 nodes results using the integration method for finding energy rejection was 4.89%, although the magnitude of the difference is similar to the preceding case (Fig. 2). Once again, the conduction method was more grid dependent.

In all of the cases evaluated in the grid study, the efficiency from the integral method for finding fin heat transfer [Eq. (17)] was found to be insensitive to numerical grid size (less than 5% variation for the worst case). Additionally, the efficiency from the base conduction method [Eq. (16)] was low at 40 nodes and converged to the integral method results as nodal network size increased. The results suggest that the integral method may be used as an accurate way to find the efficiency of a fin with a network of 40 nodes.

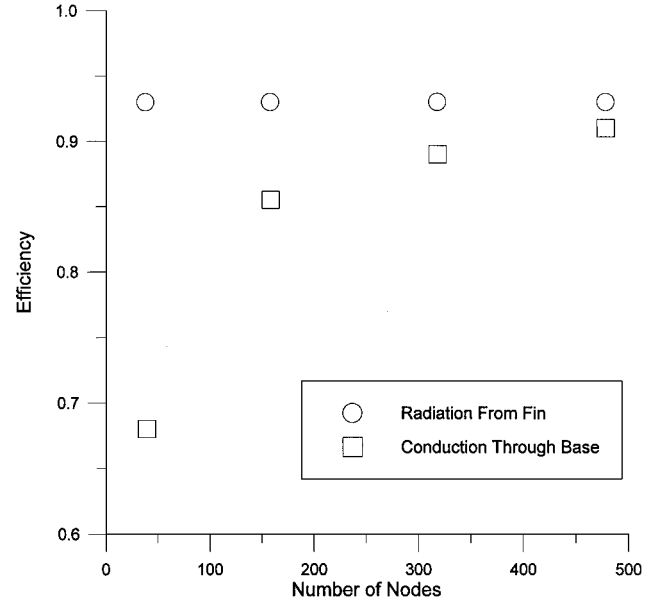

Fig. 2 Error comparison for HPP = 900, $\zeta_{HP} = 0.5$, and EP = 0.

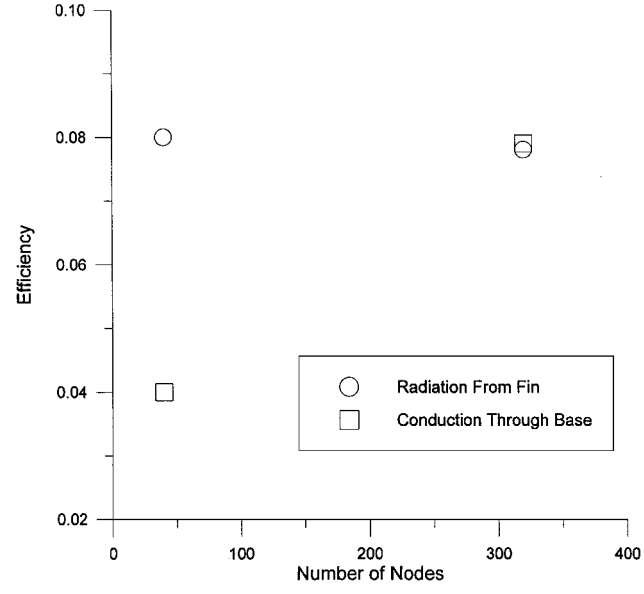

Fig. 3 Error comparison for HPP = 900, $\zeta_{HP} = 3$, and EP = 0.9.

Numerical Results

This section explores the effect of critical parameters in the numerical solution on the calculated results. This section also reports the results of the numerical solution and compares these results with previous work for standard fins. The design charts (Figs. 4–8) compare efficiencies for various combinations of profile numbers ζ_{HP}, EP, and HPP. An additional chart is included to illustrate trends occurring across the series of design charts on a consolidated graph (Fig. 9).

Results of the numerical solution were found for the following ranges of critical parameters: HPP at 0, 200, 600, 1000, and 5000; EP at 0–0.9 in increments of 0.1; and ζ_{HP} 0–3.5.

Figure 4 represents the standard fin case where HPP = 0. With HPP = 0, the relevant equations reduce the FPHPF to a solid fin with no vapor space. Mackay[14] has previously solved the equations for this condition, and so this chart was used as an initial test chart to verify that the results of this numerical derivation matched the previous work. Mackay's design chart has been plotted in Fig. 4 to show the correlation between the two models. It appears that slight deviations occur between the two plots; the largest difference was calculated to be 5%. This may be a result of manual data entry of

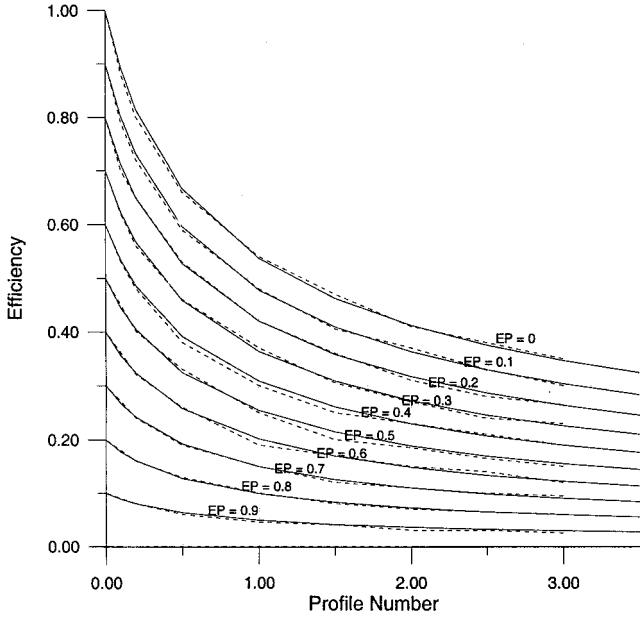

Fig. 4 Efficiency at HPP = 0 for Mackay's work[14] (– – –) and numerical solution (——).

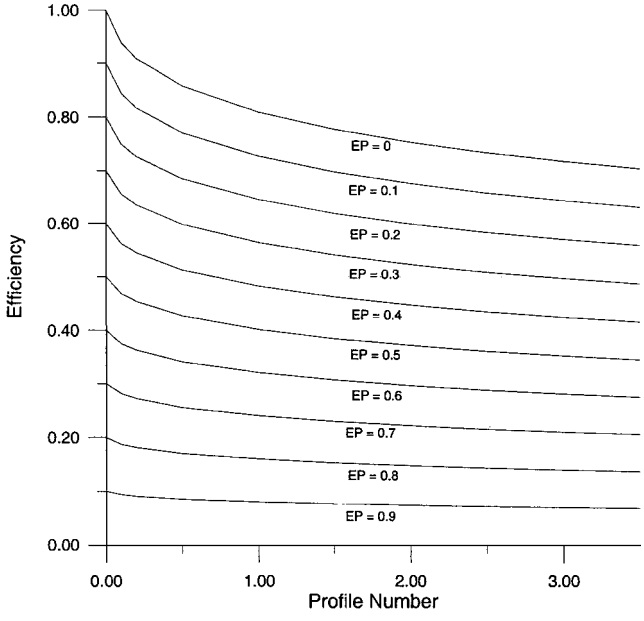

Fig. 5 Efficiency for HPP = 200.

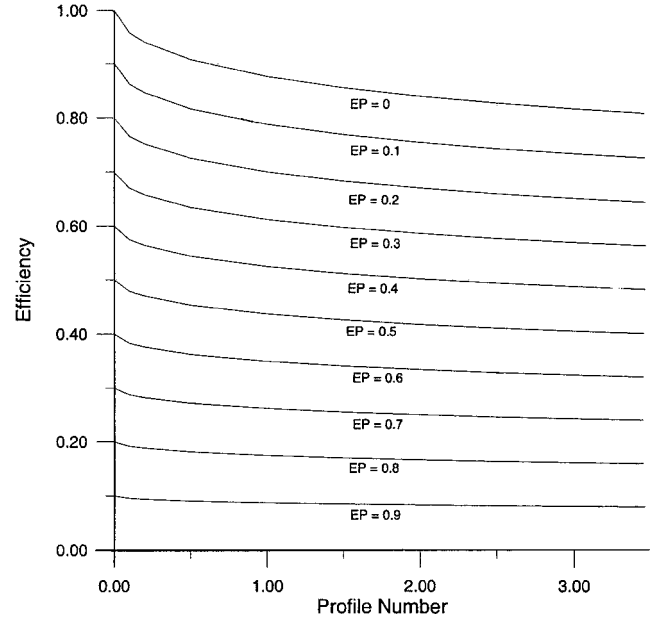

Fig. 6 Efficiency for HPP = 600.

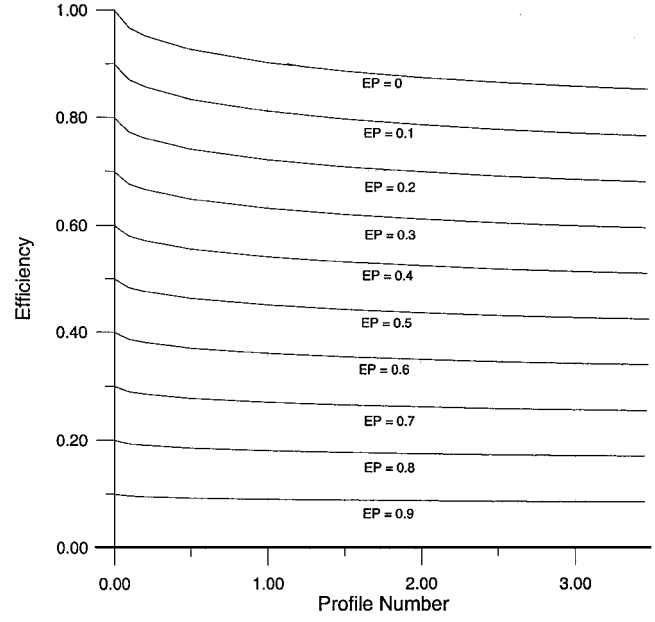

Fig. 7 Efficiency for HPP = 1000.

Mackay's plot into the graphing software. Overall, the agreement between the two models is very good.

The next four plots (Figs. 5–8) show trends in efficiency as HPP and ζ_{HP} are increased. In general, as the HPP is increased, the efficiency increases. Additionally, as ζ_{HP} increases, the efficiency decreases. Another item of interest is the effect of EP on efficiency: as EP increases, the efficiency drops by a corresponding percentage.

These charts have been provided to help the designer predict FPHPF performance. The added HPP factor calls for a third dimension in plotting, hence the multiple charts for the same values of ζ_{HP} and EP. Visual interpolations between charts are necessary for HPP values not plotted. The charts enable the FPHPF designer to determine rapidly the heat transfer capability of a proposed design by finding the factors ζ_{HP}, HPP, and EP. Figure 4 can be used to predict the standard fin performance based on the same parameters.

Figure 9 represents a new twist on the design curves. Figure 9 shows efficiency at various profile numbers, as in the other charts. This chart, however, holds the environmental parameter constant at EP = 0 and shows the effect of the various values of HPP. For comparison, another series of plots at EP = 0.9 is placed on the graph. This chart clearly shows that increases in HPP give increasingly smaller incremental increases in efficiency, although an increase always occurs.

Additionally, the plot at EP = 0.9 in Fig. 9 shows that increases in EP tend to compress the spread between different values of HPP. For example, the efficiency difference between HPP = 0 and 1000 at EP = 0 (upper plot) is roughly 52%, whereas the efficiency difference between HPP = 0 and 1000 at EP = 0.9 (lower plot) is only about 6%. Also note that the slope of the efficiency curve always increases gradually from highly negative values toward zero as the profile number increases. As the slope of the curve approaches zero, changes in profile number no longer affect the efficiency. When Eq. (5) is examined, the physical significance emerges; changes in length, thickness, temperature, radiative properties, and thermal conductivity no longer adversely affect the efficiency. This finding implies that, at higher values of ζ_{HP} and HPP, the preceding physical parameters may be altered without causing a large change in efficiency of the FPHPF.

Table 1 Summary of critical parameters for each test

	Uncharged test		Charged test 1		Charged test 2		Charged test 3	
Parameter	h_e	h_c	h_e	h_c	h_e	h_c	h_e	h_c
Effective thickness, mm	0.856	0.856	0.856	0.856	0.942	0.942	0.856	0.856
Number of wires	43	43	43	43	43	43	95	95
Wire o.d., mm	0.5	0.5	0.5	0.5	0.8	0.8	0.5	0.5
Number of grooves	4	4	4	4	4	4	4	4
Groove depth δ, mm	NA	NA	0.05	0.4	0.05	0.7	0.05	0.4
Land thickness, mm	NA	NA	0.4	0.05	0.7	0.05	0.4	0.05
Vapor radius, mm	NA	NA	1.78	1.43	1.80	1.15	0.80	0.45
Internal convection coefficient, W/(m^2 · K)	0	0	715	2329	705	2545	1595	7445
Profile number	0.346	0.346	0.346	0.346	0.314	0.314	0.321	0.321
Heat transfer, W	54.2	54.2	48.4	48.8	50.0	50.4	48.1	48.3
Efficiency, %	74.9	74.9	97.3	98.8	96.7	98.2	98.6	99.5

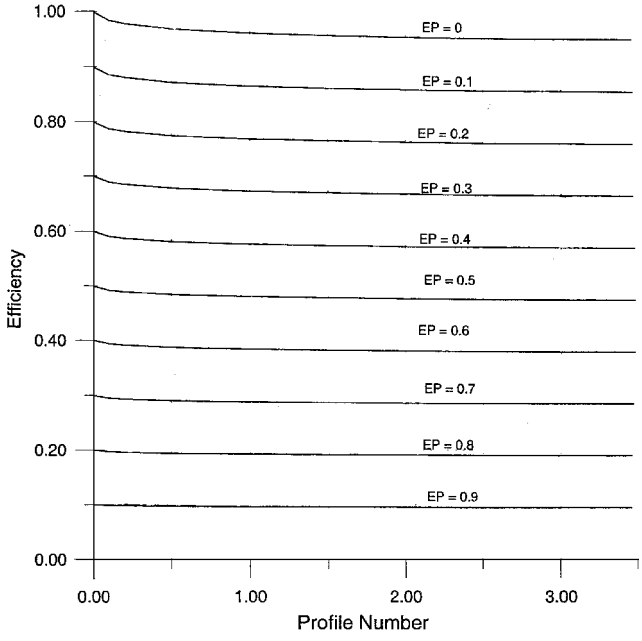

Fig. 8 Efficiency for HPP = 5000.

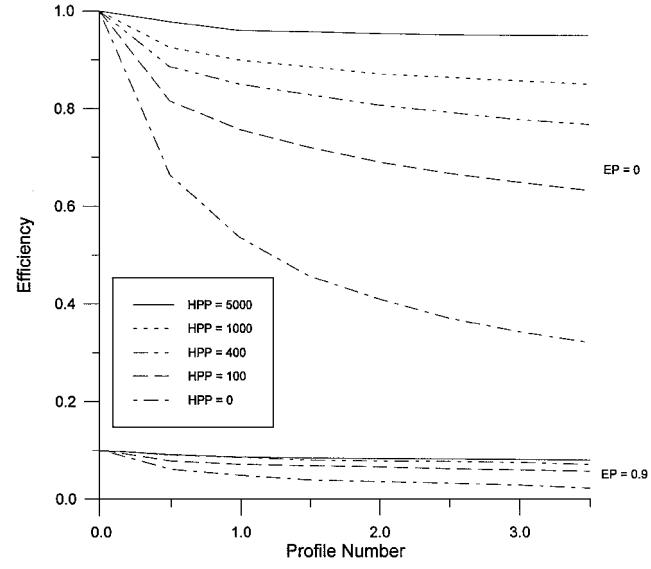

Fig. 9 Efficiency for EP = 0 and 0.9.

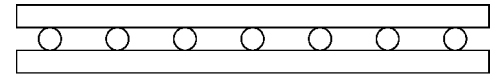

Cross-section

Fig. 10 Micro heat-pipe array with sintered wires.[16]

Comparison to Experimental Data

Wang et al.[16] studied the temperature distribution of radiator fins with embedded micro heat pipes. The fins were constructed by sintering an array of aluminum wires (0.5-mm o.d.) between two aluminum sheets (0.4 mm thick each), creating a fin measuring 152 mm^2 (see Fig. 10). Acetone was used as the working fluid.

To predict the temperature distribution using the new FPHPF model for the fin with micro heat pipes, it was necessary to input equivalent conditions. Table 1 summarizes the values of critical parameters used in the model for the different cases studied. Additionally, computed values of heat transfer and efficiency are presented for the different arrangements.

The results from the model for the uncharged fin are shown in Fig. 11. The topmost curve represents the FPHPF model results. Closely following this curve are the experimental data of the uncharged micro heat-pipe fin in the test environment by Wang et al.[16] The results closely correlate with each other. Just below the Wang et al. experimental data, the numerical model by Wang et al. follows the same trend as the previous two curves. The close agreement between the test data from Wang et al. and the FPHPF model is a good indication that the proposed model is valid for the uncharged case.

Figure 12 shows that the FPHPF model does not follow the experimental temperature distribution as closely as does the Wang et al.[16] model for the charged fin. Although the variance with the experimental data is relatively small, it is noteworthy that the temperature distribution predicted by the FPHPF model is more isothermal than the experimental data.

The second charged fin test of Wang et al.[16] was a micro heat-pipe fin with a wall thickness of 0.4 mm, an interior wire diameter of 0.8 mm, and a total of 43 wires. The results of the model are displayed in Fig. 13. The FPHPF model continues the trend seen in charged test 1 in that it is more isothermal than the experimental data would suggest. The difference between charged test 2 and test 1 was the wire diameter size (0.5 and 0.8 mm), and so this could be a factor in model inaccuracies when calculating the evaporation heat transfer coefficient h_i in the FPHPF model. Another possibility could be suboptimal filling of the test fin with working fluid, allowing for puddling in the fin on one extreme, or wick dry-out on the other extreme. If the filling conditions in the test are different from the assumptions used in the FPHPF model, a disparity will occur.

The third and final charged fin test was with a micro heat-pipe fin with a wall thickness of 0.4 mm, an interior wire diameter of 0.5 mm, and a total of 95 wires inside the fin (Fig. 14). This test had the closest correlation between the experimental data and the FPHPF model. The closer correlation between the numerical results and the experimental data could be explained by better modeling of the filling conditions.

At first glance, it might appear that this new model is less accurate than the Wang et al. model.[16] That may be true, but one point related

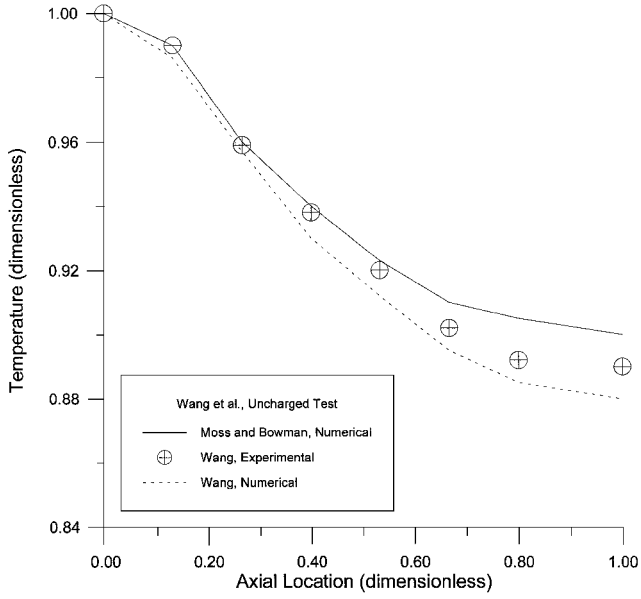

Fig. 11 Position vs temperature for Wang et al.[16] and FPHPF for the uncharged fin.

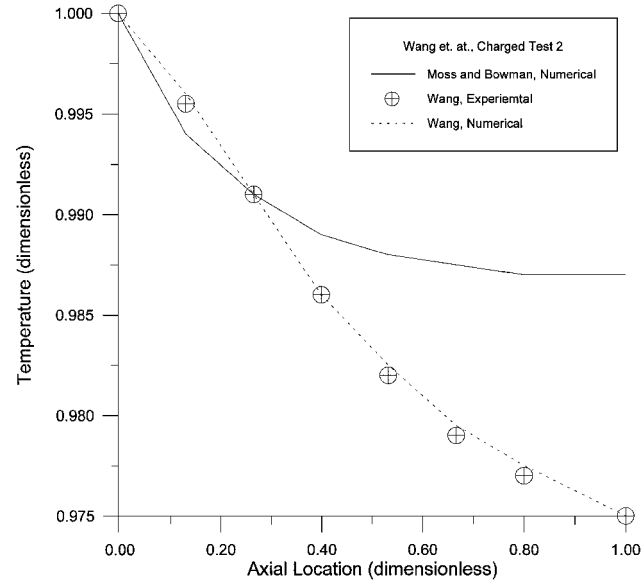

Fig. 13 Position vs temperature for Wang et al.[16] test 2 and FPHPF for the charged fin.

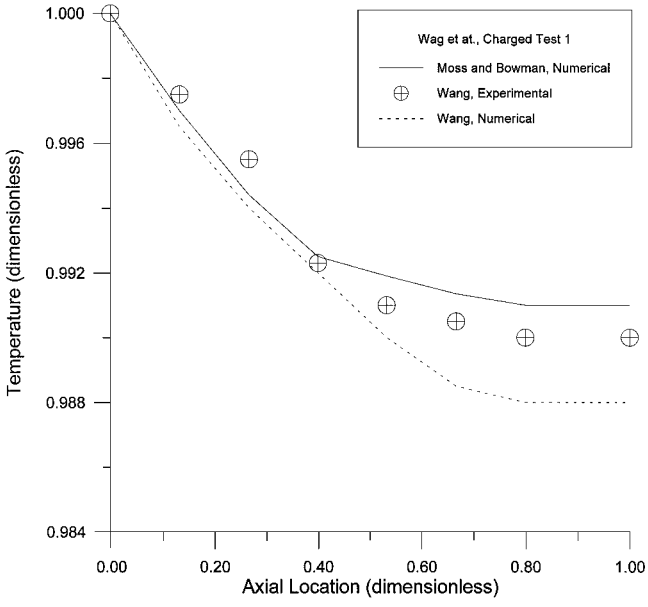

Fig. 12 Position vs temperature for Wang et al.[16] test 1 and FPHPF for the charged fin.

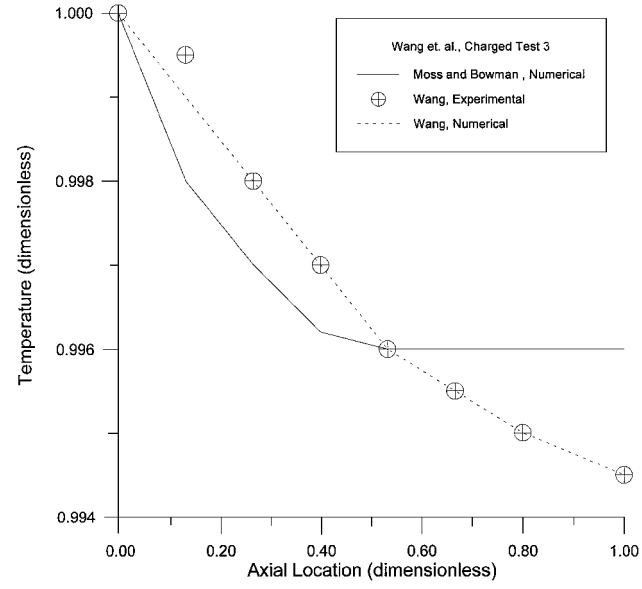

Fig. 14 Position vs temperature for Wang et al.[16] test 3 and FPHPF for the charged fin.

to the Wang et al. model must be considered. During the Wang et al. numerical simulations, the experimental fin tip temperature was used as a boundary condition to obtain the best fin parameters that gave fin temperatures that matched at the fin base and tip. For the numerical results presented by this new work, only the fin physical dimensions and base temperature were used for the numerical model. Thus, though the results may appear to be less accurate, they were obtained using less of the experimental data to fine tune the results.

FPHPF Model vs the Viking Satellite

On 20 August and 9 September 1975, NASA launched the Viking 1 and 2 satellite[17] with a goal of studying the Martian surface via an orbiter and a lander. The orbiter was powered by a radioisotope thermoelectric generator capable of 683-W thermal at beginning of life and included six cooling fins (113.8 W/fin) to dissipate the generated heat. The root temperature of the fin was set not to exceed a 395-K maximum. The generator provided energy to orbiter instruments for imaging, infrared thermal mapping, atmospheric water detection, and radio wave detection.

How much better (or worse) would the cooling fins have performed if NASA had used a series of six FPHPFs instead of the standard fins? How much less would the satellite have weighed using FPHPFs, enabling the satellite to carry additional instrumentation? Could the RTG have been made more powerful because the FPHPFs could dissipate more energy to the environment? To answer these types of questions, the FPHPF model was put to the test against the standard fins of the Viking satellite. It was postulated that use of FPHPFs instead of the standard fins would improve performance.

In performing the comparison, the following assumptions were made, based on interpretations of Fig. 15 and on likely fin materials: aluminum as the fin material [$k = 237$ W/(m · K)], fin length of 28 cm, height of 20 cm; base thickness of 0.5 cm, tip thickness of 0.1 cm, average thickness of 0.3 cm, and emissivity $\varepsilon = 0.9$.

To determine the heat transfer from the Viking fin, the parameters were entered into the FPHPF model for a fin with a thickness of 3 mm (average of the Viking fin) and other dimensions as given earlier. The model returned an efficiency of 59.9% at $\zeta_{HP} = 0.72$. With Fig. 4 used for a standard fin, EP was found to be around 0.04. Under these conditions, the heat transfer was calculated to be 83.6 W. For six

Table 2 FPHPFs; same heat transfer as Viking fins

Parameter	Values		
EP	0.04	0.04	0.04
HPP	0	100	5000
ζ_{HP}	0.719	<3.5	<3.5
Efficiency, %	60.0	62.0	91.0

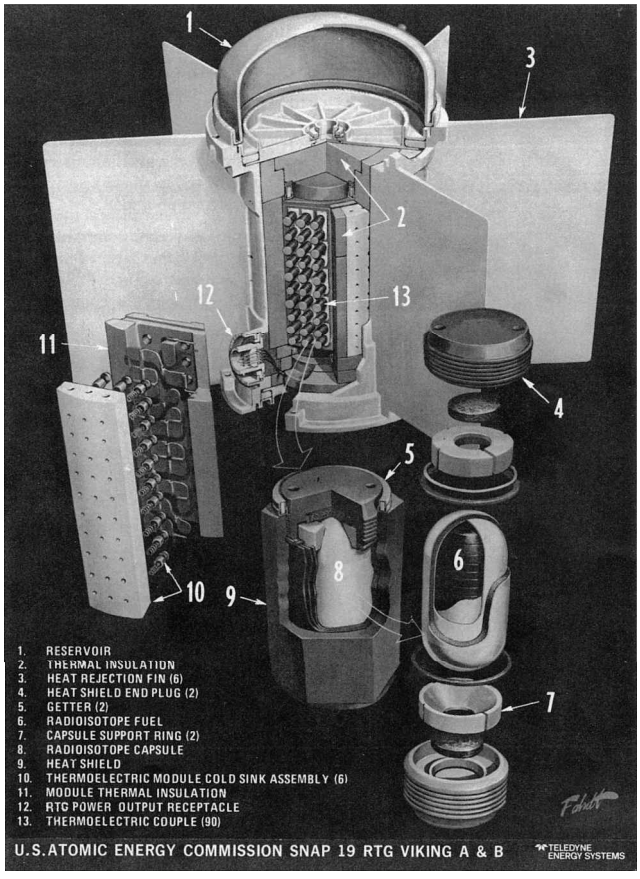

Fig. 15 Graphic of Viking SNAP-19 RTG.[17]

fins, this comes to only 518 W, whereas the total heat generated by the RTG was 683 W. This difference can be attributed to radiation from the cylindrical surface of the RTG (Fig. 15), which had a high-emissivity coating to enhance heat transfer.[17] Thus, for the purposes of the following scenarios, the required heat transfer per fin was set to 83.6 W.

Two scenarios were considered. The first compared the Viking solid fins on the RTG to an RTG with the same number of FPHPFs with variable values of ζ_{HP} and HPP, as long as the heat transfer and height remained the same and the length of the fin was less than or equal to that of the Viking fin. The purpose of the test was to determine the range of these values that would give efficiencies greater than, or equal to, that of the Viking fin. The second scenario assumed the same number of fins and the same amount of heat radiated as in the Viking case (86.3 W/fin) but with FPHPFs of HPP = 5000, similar to those of Wang et al.[16] The purpose of this scenario was to determine the decrease in mass of the new fins over the Viking fins, as well as the changed length.

Results from the scenarios are displayed in Table 2. The first scenario examined the range of values of the three critical parameters (EP, HPP, and ζ_{HP}) for an FPHPF with HPP = 100 and 5000. When these extreme endpoints were examined, it was hoped that trends in ζ_{HP} and efficiency would appear. As was stated earlier, EP = 0.04 was held constant for all fins because the value is independent of the presence of a heat pipe within the fin.

From Table 2, one can see that to achieve the same efficiency as the Viking fin, the FPHPF may have a higher ζ_{HP}. For HPP = 100, the efficiency is only slightly higher, implying that the length may not be altered greatly to achieve the same heat transfer. On the other hand, at HPP = 5000, similar to the Wang et al.[16] fin, the minimum efficiency given in the design charts is 91% at $\zeta_{HP} = 3.5$. This implies that, at the same base temperature, this fin may be shorter and lighter.

The second scenario examined a set of six FPHPFs at HPP = 5000 and six Viking fins on the basis of weight and length. The set of fins on the Viking orbiter weighed 2.72 kg, whereas the FPHPF weighed only 0.62 kg, or 77.2% less, while dissipating the same amount of heat to the environment as the Viking fins. The difference in mass comes mainly from the vapor space and the liquid-saturated wick, which are less dense than solid aluminum.

Fin length for the same heat transfer was the second important criterion for comparison. The Viking fin had a length of 28 cm, whereas the FPHPF may dissipate the same thermal energy at a length of only 18.4 cm, a 34.3% decrease in length. The reason that the fin may be shortened is the increase in efficiency, which allows for decreased surface area to dissipate the same amount of energy.

Conclusions

This project has been an effort to create a design tool for the evaluation of potential designs for FPHPFs used as space radiators. The fin temperature distribution was found from an energy balance. The solution to the differential equation for the temperature distribution was found using the finite difference method. From this solution, the heat transfer from the fin was found. Once the heat transfer was determined, the efficiency of the fin was calculated. The resulting efficiencies were then plotted, based on the following three parameters: 1) profile number ζ_{HP}, 2) HPP, and 3) EP.

From the analysis, the following conclusions were reached concerning the design of the FPHPF: 1) heat-pipe radiator fins are, in general, more efficient than standard radiator fins for the same ζ_{HP} and EP; 2) heat-pipe radiator fins, in general, have less mass than standard radiator fins for the same amount of heat transferred; 3) the heat-pipe radiator fin is not necessarily superior to the standard radiator fin in terms of heat transfer; and 4) as ζ_{HP} and HPP increase, the change in efficiency decreases, meaning that the design is less constrained by the parameters and concessions may be made in the design without loss of efficiency.

Possibilities for further research should be explored. Although not exhaustive, the following is a list of suggestions:

1) Derive equations for standard fin performance with nonuniform cross-sectional areas. Study how performance is affected by varying cross-sectional area.

2) Determine whether an optimal efficiency-to-profile number ratio exists.

3) The efficiency curves appear to approach an asymptote as HPP and ζ_{HP} increase. If this is actually the case, determine the implications for the FPHPF designer as far as critical constraints are concerned.

References

[1]Chi, S. W., *Heat Pipe Theory and Practice*, 1st ed., Hemisphere, Washington, DC, 1976, pp. 1–29.

[2]Peck, S. J., and Fleischman, G. L., "Lightweight Heat Pipe Panels for Space Radiators," *Proceedings of the Sixth International Heat Pipe Conference*, Begell House, New York, 1987, pp. 362–367.

[3]Boo, J. H., and Hartley, J. G., "Analysis of the Thermal Performance of Heat Pipe Radiators," *Heat Transfer in Space Systems*, HTD-Vol. 135, American Society of Mechanical Engineers, New York, 1990, pp. 25–32.

[4]Ogushi, T., Murakami, M., Takada, T., Yao, A., Sakurai, Y., and Masumoto, H., "Experimental Investigation of a Flat-Plate Heat Pipe and Cold Plates in Thermal Management System Under Microgravity Environment," AIAA Paper 91-1360, June 1991.

[5]Baker, K. W., and Lund, K. O., "Effects of Anisotropic Conduction and Heat Pipe Interaction on Minimum Mass Space Radiators," NASA TM-105297, April 1992.

[6]Juhasz, A. J., and Peterson, G. P., "Review of Advanced Radiator Technologies for Spacecraft Power Systems and Space Thermal Control," NASA TM-4555, June 1994.

[7]Juhasz, A. J., and Rovang, R. D., "Composite Heat Pipe Development Status: Development of Lightweight Prototype Carbon–Carbon Heat Pipe with Integral Fins and Metal Foil Liner," NASA TM-106909, May 1995.

[8]Peterson, G. P., *An Introduction to Heat Pipes: Modeling, Testing, and Applications*, 1st ed., Wiley, New York, 1994, pp. 285–322.

[9]Dunn, P. D., and Reay, D. A., *Heat Pipes*, 2nd ed., Pergamon, London, 1978, pp. 255–290.

[10]Faghri, A., *Heat Pipe Science and Technology*, 1st ed., Taylor and Francis, Washington, DC, 1995, pp. 41–55.

[11]Ogushi, T., Murakami, M., Masumoto, H., and Hayashi, R., "Study on Newly Developed Flat Plate Type Heat Pipe Heat Sink," *Proceedings of the 1988 National Heat Transfer Conference*, Vol. 1, American Society of Mechanical Engineers, New York, 1988, pp. 517–521.

[12]Um, J.-Y., Chow, L. C., and Baker, K., "An Experimental Investigation of Flat Plate Heat Pipe," *Fundamentals of Heat Pipes*, HTD-Vol. 278, American Society of Mechanical Engineers, New York, 1994, pp. 21–26.

[13]Moss, T. W., and Bowman, W. J., "Efficiency of a Constant Area, Adiabatic Tip, Heat-Pipe Fin," AIAA Paper 99-3443, June 1999.

[14]Mackay, D. B., *Design of Space Powerplants*, Prentice–Hall, Englewood Cliffs, NJ, 1963, pp. 28–50.

[15]Bowman, W. J., Storey, J. K., and Svensson, K. I., "Analytical Comparison of Standard and Heat Pipe Fins," AIAA Paper 99-0475, Jan. 1999.

[16]Wang, Y. X., Ma, H. B., and Peterson, G. P., "Investigation of the Temperature Distribution in Radiator Fins with Micro Heat Pipes," AIAA Paper 2000-0969, Jan. 2000.

[17]Angelo, J., and Buden, D., *Space Nuclear Power*, 1st ed., Orbit, Malabar, FL, 1985.

T. C. Lin
Associate Editor